



MULTI-AXIAL REAL-TIME HYBRID SIMULATION TESTING

A. Najafi⁽¹⁾, B. F. Spencer Jr.⁽²⁾

⁽¹⁾ Doctoral candidate, Department of Civil and Environmental Engineering, University of Illinois at Urbana-Champaign, Urbana, IL, anajafi2@illinois.edu

⁽²⁾ Professor, Department of Civil and Environmental Engineering, University of Illinois at Urbana-Champaign, Urbana, IL, bfs@illinois.edu

Abstract

Dynamic laboratory testing is an integral part of our understanding of the performance of structural systems under earthquake loading. The two main approaches for dynamic testing have been shake table and pseudo-dynamic (PsD) methods. The shake table approach typically uses servo-hydraulic means to excite a moving base and an onboard structural system. The limitation of the shake table method is that large tables are expensive to build and operate, and the scaling necessary to satisfy the similitude laws in smaller tables is a challenging task. The PsD approach avoids the need for testing of the complete structure, and instead partitions structural systems into numerical and physical components, for a more space- and cost-effective testing method. Damping and inertial forces are calculated numerically, and displacements are executed on the physical structure to obtain the restoring forces. The slow application of the displacements results in negligence of time-dependent material effects.

Real-time hybrid simulation (RTHS) is an alternative to shake table and PsD approaches for studying the seismic behavior of structural systems. Structures are divided into numerical and physical component, but instead are tested in real-time. Restoring, damping, and inertial forces are all accounted for in the physical execution as a result of the real-time testing. Additionally, rate-dependent and nonlinear material effects are also incorporated in the physical testing. For a realistic replication of seismic conditions in laboratory settings, multi-axial RTHS capabilities are often desired. In these experiments, multi-axial boundary conditions made up of multiple actuators are necessary to test the physical specimen. Significant coupling can be present between the actuators in such setups. Kinetic transformations are necessary to operate each actuator for achieving desired boundary condition deformations. Furthermore, appropriate compensation must be provided to the reference trajectory, as actuators tend to add unwanted dynamics to the RTHS experiments. In this paper, an RTHS framework is introduced for multi-axial testing. The framework discusses important hardware and programming features that are necessary for a successful multi-axial RTHS testing. The successful results for a multi-span curved bridge experiment are presented, where one bridge pier is physically tested while the remaining piers and the curved deck are numerically modeled.

Keywords: Real-time hybrid simulation, multiple-actuator, dynamic coupling, actuator compensation, multi-span curved bridge



1. Introduction

Laboratory testing of structures allows researchers to develop better building standards and codes for dealing with large earthquakes. Some of the most common methods for testing structural response to earthquake loadings are: (i) shake table testing, (ii) pseudo-dynamic (PsD) testing, and (iii) real-time hybrid simulation (RTHS). The shake table approach uses a moving platform to excite a small- or full-scale structure, depending on the size of the table. The limitations on the shake table method are the table size, restriction to base excitation, and high cost of operations for the big tables. The scaling of the dynamic performance from small-scale models to full-scale is also a difficult task. The pseudo-dynamic method was proposed as an alternative to shake table testing. Introduced by Hakuno et al. [1] and Takanashi et al. [2], the PsD involves application of quasi-static load equivalent of the inertial forces calculated analytically, onto the physical specimen.

Realistic structural testing, necessitates a shift toward incorporation of real physical conditions, including application of structural loads at real velocities and through three-dimensional means. Nakashima et al. [3] introduced real-time pseudo-dynamic testing with numerical calculations, physical testing and data acquisition systems performed at a sampling frequency of 1000 Hz. With the availability of fast and affordable modern computers, hardware and data acquisitions systems, more researchers are developing RTHS solutions [4], [5]. RTHS with multiple actuators and axes has also been the subject of research, due to the realism and breadth of applications it enables [6], [7]. Fernandois and Spencer [8] introduced a 6 degree-of-freedom (DOF) RTHS framework for multi-axial boundary conditions. Experiments on a steel moment frame demonstrated the capabilities of the proposed multi-axial framework, however with some stability limitations. Numerous challenges remain unsolved in the multi-axial RTHS domain, including actuator compensation (i.e., force control), kinematic transformations and more sophisticated numerical modeling techniques.

This paper introduces a multi-axial RTHS framework for experimenting on multi-axial boundary conditions. This framework consists of procedures for actuator compensation, kinematic transformation, and data acquisition, necessary for a successful multi-axial RTHS implementation. A new decoupled control scheme is introduced, which ensures ease of design and overcomes the stability issues in previous developments. A multi-span curved bridge structure is selected for verification of the proposed framework, where one pier is physically tested, and the remainder of the structure is numerically solved using finite elements. Results demonstrate successful implementation of the proposed framework.

2. Multi-axial RTHS

A multi-axial RTHS experiment may have one or multiple physical substructures, and a numerical model represented via the equation of motion:

$$\mathbf{M}_N \ddot{\mathbf{x}}_N + \mathbf{C}_N \dot{\mathbf{x}}_N + \mathbf{K}_N \mathbf{x}_N = \mathbf{f}_{EXT} - \mathbf{f}_{RES} \quad (1)$$

where \mathbf{M}_N , \mathbf{C}_N , and \mathbf{K}_N are mass, damping and stiffness property matrices, and $\ddot{\mathbf{x}}_N$, $\dot{\mathbf{x}}_N$, and \mathbf{x}_N are the acceleration, velocity, and displacement vectors of the RTHS numerical model. The inertial earthquake forces and restoring forces from the physical specimen are described by \mathbf{f}_{EXT} and \mathbf{f}_{RES} , respectively. Restoring forces are measured via load cells at the boundary condition with physical specimen.

In this section, a multi-axial RTHS framework is introduced for multi-axial boundary conditions, such as the 6-DOF shake tables found in numerous institutions and Load and Boundary Condition Boxes (LBCBs) at the University of Illinois at Urbana-Champaign. A multi-axial boundary condition typically has a *fixed base* and a *moving base*, and several prismatic servo-hydraulic actuators connecting the two, as shown in Fig 1. \mathbf{R}_f and \mathbf{R}_m are two *reference frames* selected on the fixed and moving bases, respectively. The physical specimen is attached to the boundary condition at \mathbf{R}_m . \mathbf{v} is the translation vector between the two reference frames, \mathbf{a}_i is a vector from the fixed reference frame to the i^{th} actuator joint on the fixed platform, \mathbf{b}_i is a vector from the moving reference frame to the i^{th} actuator joint on the moving platform, and \mathbf{s}_i is a vector representation of the actuator length.

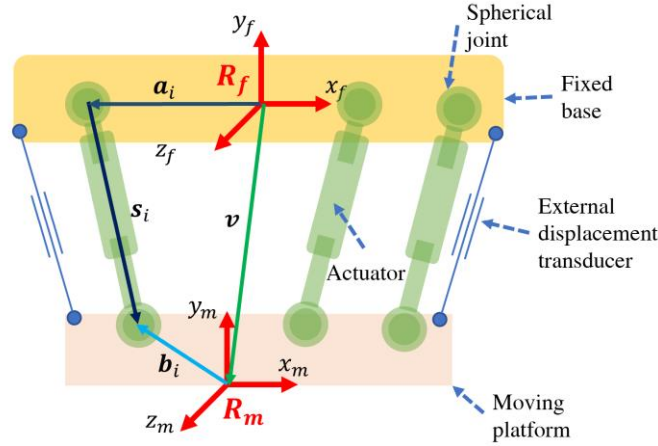


Fig. 1 – Multi-axial boundary condition kinematics

2.1 Kinematics of multi-axial boundary conditions

For some rotational matrix $\mathbf{A}(\theta_x, \theta_y, \theta_z)$, describing the rotational movement of the moving platform in three-dimensions, and translational vector $\mathbf{v} = \{u_x, u_y, u_z, \theta_x, \theta_y, \theta_z\}^T$, the following formulation describes the i^{th} actuator vector length:

$$\mathbf{s}_i = \mathbf{v} + \mathbf{A}\mathbf{b}_i - \mathbf{a}_i \quad (2)$$

$$q_i = |\mathbf{s}_i| = f_i(\mathbf{v}) \quad (3)$$

where q_i is the total actuator length and f_i is the particular nonlinear function. An equivalent formulation is also developed for describing the i^{th} displacement transducer vector length:

$$\boldsymbol{\sigma}_i = \mathbf{v} + \mathbf{A}\boldsymbol{\beta}_i - \boldsymbol{\alpha}_i \quad (4)$$

$$\rho_i = |\boldsymbol{\sigma}_i| = g_i(\mathbf{v}) \quad (5)$$

where $\boldsymbol{\sigma}_i$ is the vector length of the external transducer, and $\boldsymbol{\alpha}_i$ and $\boldsymbol{\beta}_i$ are vectors from reference frames to transducer joints. In Eq. (5), ρ_i is the total displacement transducer length and g_i is the corresponding nonlinear function. Obtaining Cartesian motion from actuator or transducer lengths involves inverting Eqs. (3) and (5), and solving implicit nonlinear equations, which is unachievable for rapid calculation speeds required for RTHS testing. This inversion can be simplified through linearized approximation around the equilibrium point $\mathbf{v} = \mathbf{0}$, resulting in:

$$\dot{q}_i = \mathbf{J}_f \dot{\mathbf{v}} \quad (6)$$

$$\dot{\rho}_i = \mathbf{J}_g \dot{\mathbf{v}} \quad (7)$$

where \mathbf{J}_f and \mathbf{J}_g are Jacobian matrices, and \dot{q}_i , $\dot{\rho}_i$, and $\dot{\mathbf{v}}$ are derivatives of the terms described earlier. These Jacobians are next used to obtain incremental changes in Cartesian motion.

$$\mathbf{v}_{k+1} = \mathbf{v}_k + \mathbf{J}_f (q_{k+1} - q_k) \quad (8)$$

$$\mathbf{v}_{k+1} = \mathbf{v}_k + \mathbf{J}_g (\rho_{k+1} - \rho_k) \quad (9)$$

Since loadcells are typically in line with the actuator arms, the following transforms actuator forces to Cartesian forces:

$$\mathbf{P}_{cart} = \mathbf{J}_f^T \mathbf{P}_{act} \quad (10)$$

where \mathbf{P}_{cart} and \mathbf{P}_{act} represent the Cartesian and actuator force vectors.



2.2 Multi-axial RTHS framework

The multi-axial framework is divided into four processes: (i) numerical model, (ii) numerical-to-physical (N2P) transformation, (iii) physical testing, and (iv) physical-to-numerical (P2N) transformation. The N2P transformation converts Cartesian target boundary conditions to actuator control signals, and P2N transformation converts actuator forces to Cartesian restoring forces. *Inverse kinematic transformation* (IKT) is used for transforming Cartesian, to actuator or external transducer motions. *Forward kinematic transformation* (FKT) transforms actuator and potentiometer motion to Cartesian coordinates. The architecture of the proposed multi-axial RTHS framework is illustrated in Fig. 2.

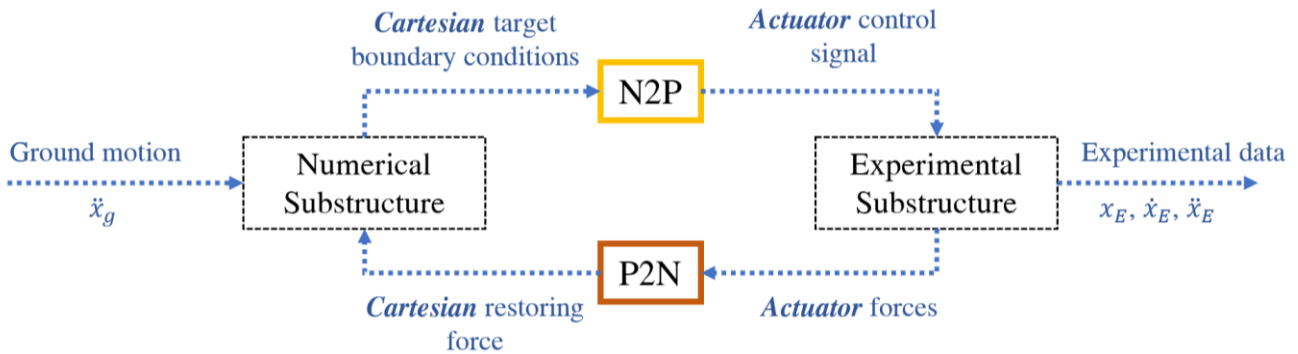


Fig. 2 – Proposed multi-axial RTHS framework

Experimental substructures are typically equipped with external displacement transducer or other displacement transducers, installed at the position of the boundary condition. The N2P process converts Cartesian targets to actuator targets $\mathbf{r}(t)$, via a *Target IKT* process described by Eq. (3). Measured displacements are also converted via a *Transducer FKT* process, described by Eq. (9), to Cartesian coordinates, and then an *Actuator IKT* described by Eq. (3), to actuator measurements $\mathbf{y}(t)$. Actuator targets and measurements are modified via a decoupled controller algorithm, discussed in the next section, to produce the actuator control signals $\mathbf{u}(t)$. The P2N process converts loadcell measured forces via the *Force Transform*, described by Eq. (10) to Cartesian restoring forces. The N2P and P2N processes are illustrated in Fig. 3 and Fig. 4.

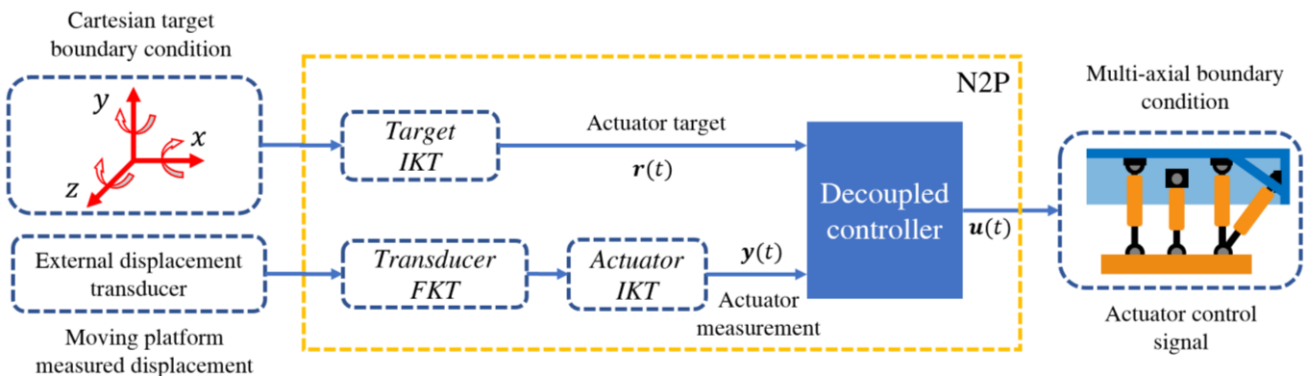


Fig. 3 – Numerical to physical process

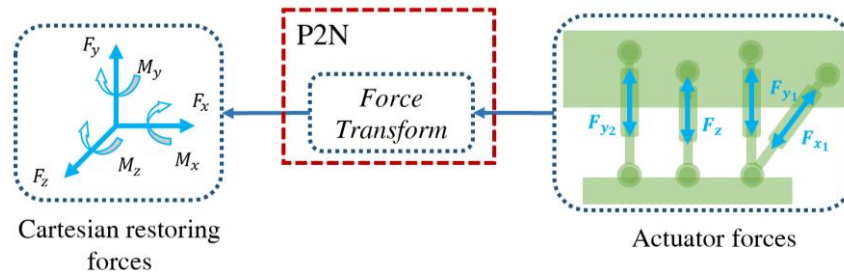
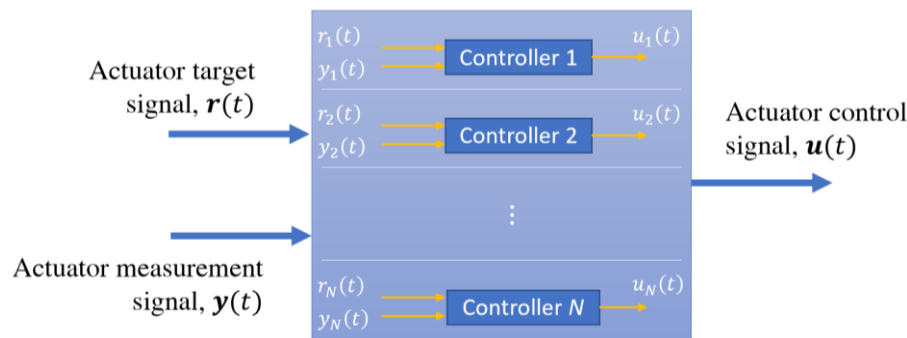


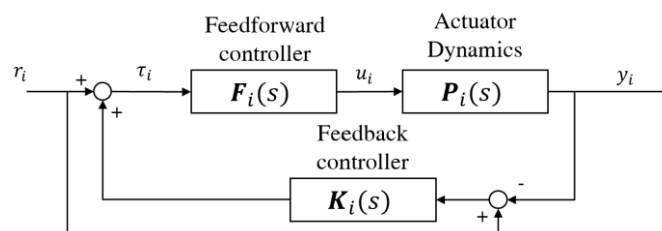
Fig. 4 – Physical to numerical process

2.3 Decoupled controller

Servo-hydraulic actuators often introduce unwanted dynamics to the target boundary condition trajectories, including actuator delays. Multi-axial boundary conditions often have multiple actuators for imposing multi-DOF displacements and forces on a physical specimen. Delays in each actuator channel results in the introduction of negative damping, which can render multi-axial RTHS tests unstable [9]. Compensation for the dynamics of multi-actuator boundary conditions may be conducted via: (i) coupled control, or (ii) decoupled control. Coupled controllers treat the multi-actuator system as a multi-input multi-output (MIMO) system where the dynamics of two or more actuators are coupled. Decoupled controllers treat each actuator as an independent single-input single-output (SISO) system. In systems with light dynamic coupling between the actuators, decoupled (SISO) controllers are recommended for ease of design and better robustness. For a multi-axial boundary condition with a total of N actuators, a decoupled controller is thus proposed per Fig. 5.

Fig. 5 – Decoupled controller for N actuator channels

The modified Model-Based Controller (mMBC) is selected for each channel of the decoupled controller. Model-based class of controllers require frequency-domain based system identification of each actuator channel and development of feedforward and feedback controllers [10]. The steps necessary for system identification of multi-axis boundary conditions are described in [11]. Fig. 6 describes the mMBC algorithm that can be applied to the i^{th} actuator channel of the multi-axis boundary condition. $P_i(s)$, $F_i(s)$, and $K_i(s)$ represent the actuator dynamics, feedforward and feedback controllers, respectively. r_i and y_i are the i^{th} actuator reference and measured signals, respectively.

Fig. 6 – Controller for the i^{th} actuator channel



3. Experimental Verification

In this section, the experimental setup for verification of the proposed multi-axial RTHS framework are described. A 1/5th-scale Load and Boundary Condition Box (LBCB) at the University of Illinois at Urbana-Champaign is used as the multi-axial boundary condition. The LBCB is comprised of six servo-hydraulic actuators, each with an inline loadcell and a linear variable differential transformer (LVDT). Six external potentiometers are used for more accurate displacement measurements. Details regarding the force and stroke capacities of the 1/5th-scale LBCBs are found in Najafi et al. [11].

A host PC is used with a MATLAB/Simulink Real-Time Workshop. Simulink Coder converts Simulink models to C++ source code. Source codes are uploaded to a Speedgoat performance real-time target machine (i.e., microcontroller). Measurement and control signals are transmitted through the analog IO interface of the microcontroller to a Shore Western servo-controller, which handles inner-loop controller tasks including PID control. Fig. 7 demonstrates the physical setup and hardware loop used in this verification study.

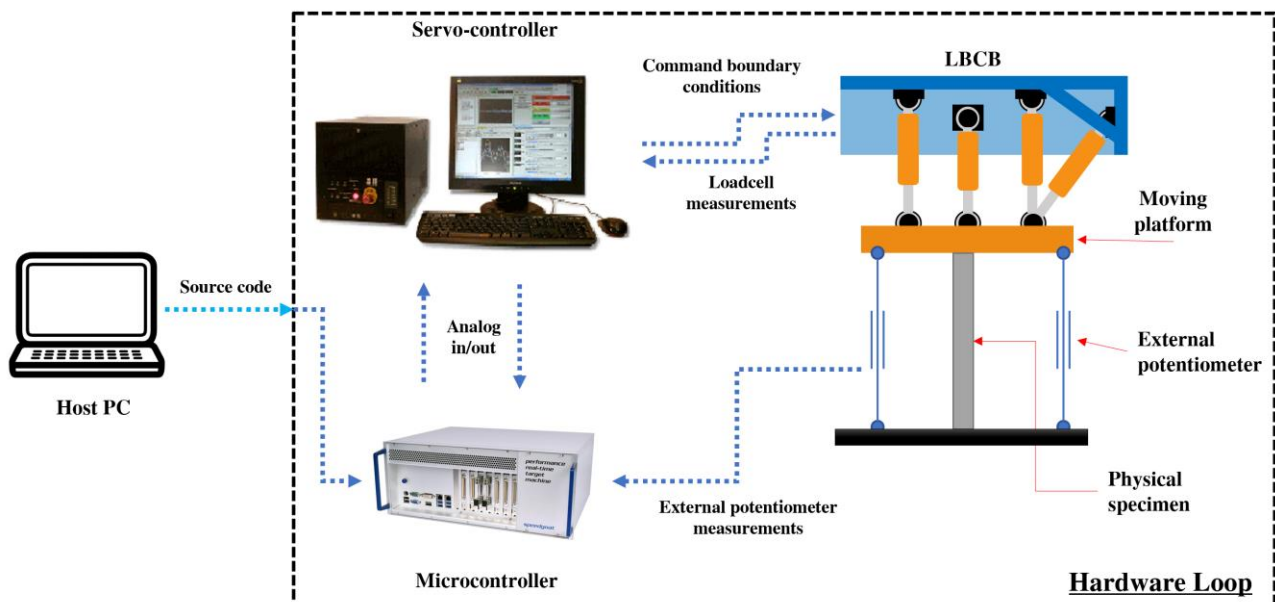


Fig. 7 – Multi-axial RTHS hardware loop

3.1 Ground motion excitation

A bi-directional ground motion (X and Y directions) is used as the excitation source, with the 1940 El Centro earthquake selected for this purpose. The excitation is PGA-scaled to 20% in the X-direction, and 10% in the Y-direction. Fig. 11(a) demonstrates the amplitude-scaled El Centro earthquake. Fig. 11(b) is power-spectral density (PSD) plot of the El Centro motion showing the energy distribution of the signal in frequency domain.

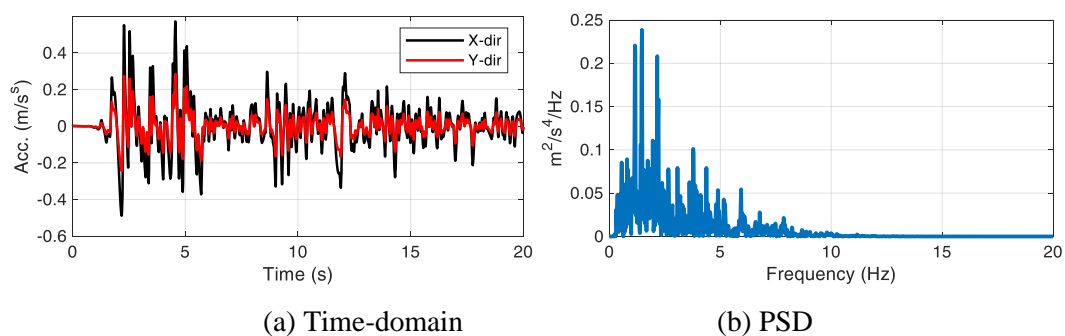


Fig. 8 – 1940 El Centro earthquake scaled in amplitude



3.1 Multi-axial RTHS Test

For the experimental verification of the proposed multi-axial RTHS framework, a multi-span curved bridge, based on prior studies discussed by Frankie et al. [12], is selected. Curved bridge decks experience large torsional forces, and axial and rotational effects are significant in all directions. The selected bridge has 4 spans, and 3 piers. The deck has a radius of 1005 mm, length of 6096 mm, with each span having the lengths: (i) span #1: 1143 mm, (ii) span #2: 2286 mm, and (iii) span #3: 1524 mm. The piers have heights of: (i) 457 mm, (ii) 570 mm, and (iii) 343 mm. Because this is a verification study, steel is selected as the bridge material, due to ease of design and simple sectional properties. For the purpose of multi-axial RTHS testing, the first pier of the bridge is physically tested, while all other elements are numerically simulated. Fig. 8(a) illustrates the curved bridge.

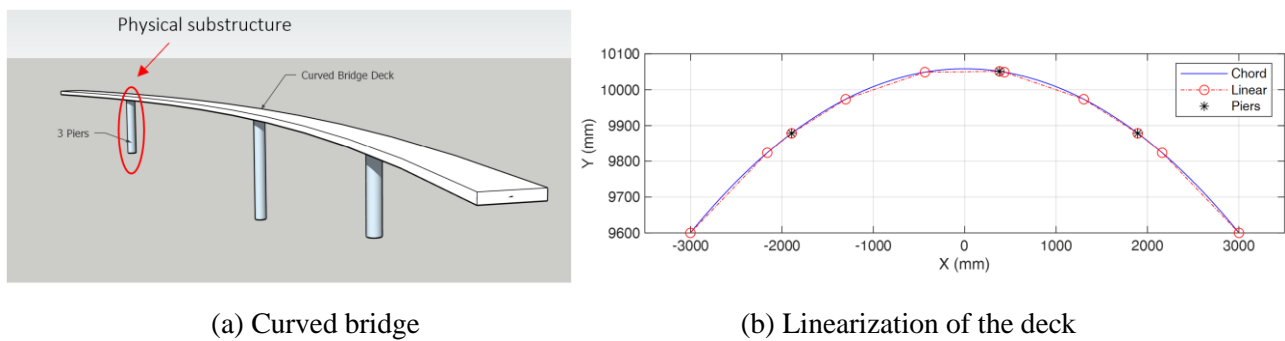


Fig. 9 – Multi-span curved bridge

For ease of numerical modeling, the curved deck is divided into 10 linear segments. The configuration of the linearized segments are shown in Fig. 8(b). To verify that the 10 linear segments are sufficient for modeling of the curved deck, the eigenvalues of the structure are compared with an identical structure with a curved deck divided into 100 linear segments. With smaller linearized segments, the performance of the approximated bridge deck will more closely match with the performance of the actual curved deck. The natural frequencies for the first 30 eigenvalues of the two structures are illustrated in Fig. 9. The first 20 eigenvalues, corresponding to a frequency bandwidth of 0-10 Hz, are closely matching. Since most of the energy of the ground motion is also in the 0-10 Hz bandwidth, per Fig. 11(b), it is deduced that the 10 linearized segments are sufficient for obtaining an accurate enough numerical model.

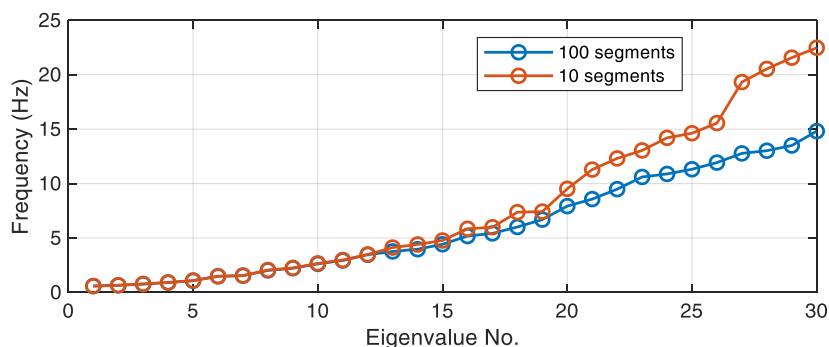


Fig. 10 – Eigenvalue comparison for the curved-bridge structure

An equivalent round steel section with a diameter of 40 mm, is assumed for the elements in the numerical substructure of the RTHS (i.e., curved deck and the piers). The physical substructure is a round steel pier with a diameter of 31.75 mm and a height of 457 mm, shown in Fig. 10. The results for the 6 DOFs shown are discussed in the next section.

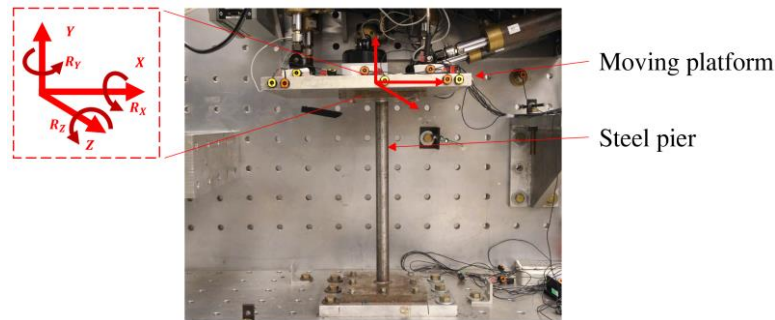


Fig. 11 – Physical substructure: steel pier

4. Results

Following execution of a multi-axial RTHS test, the six DOF behavior at the top of the physical pier (shown in Fig. 10) are discussed in this section. DOFs X , Y , and Z represent the translations at the top of the pier, and DOFs R_X , R_Y , and R_Z represent the rotations. Because of the very high axial stiffness of the physical pier, the DOF in the Y direction is fixed during the RTHS implementation to avoid damaging the actuators onboard the LBCB. Fig. 12 demonstrates the time histories each DOF following a multi-axial RTHS test.

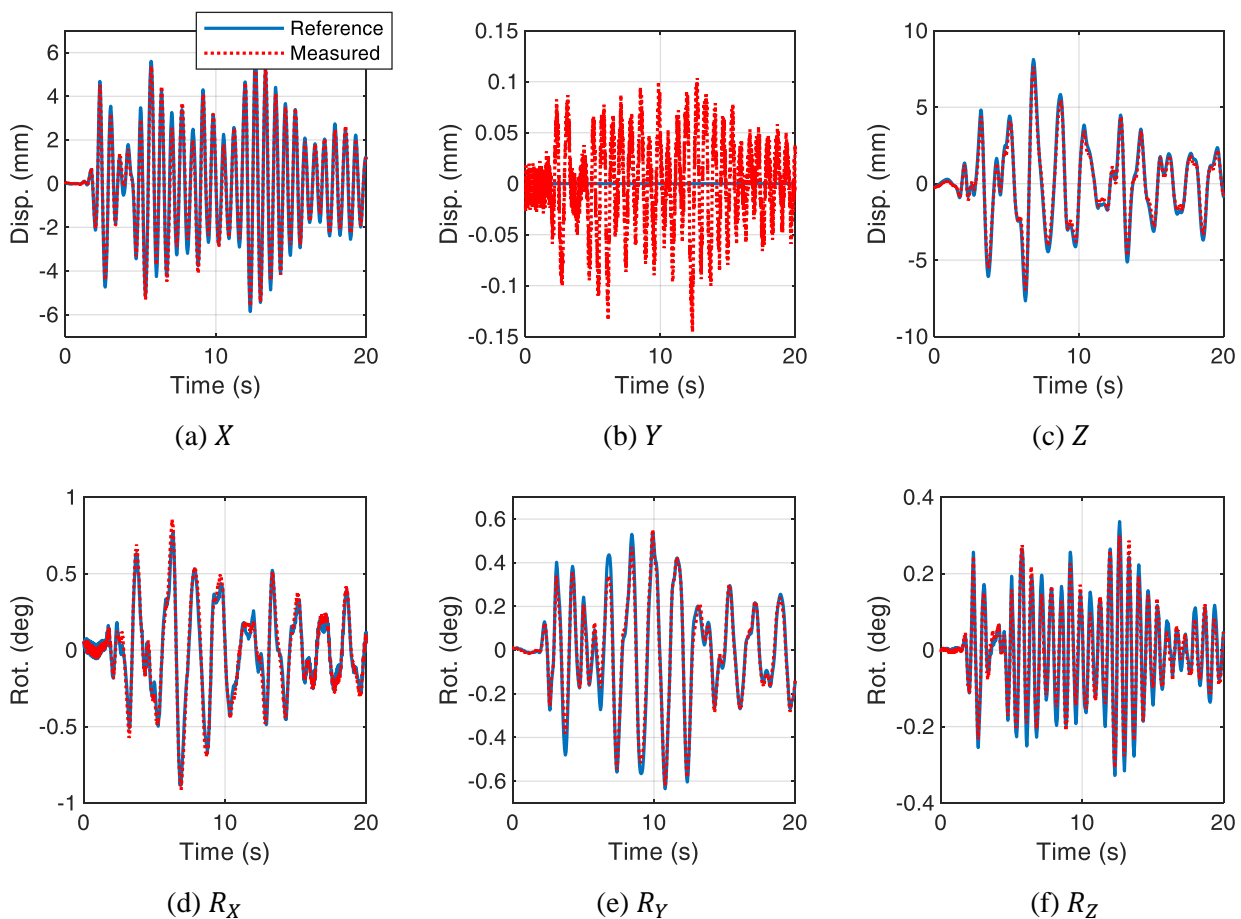


Fig. 12 – Time histories of the 6 DOFs at the top of the physical pier

The results presented illustrate the reference and measured Cartesian boundary conditions. Fig. 13 illustrates the synchronization plots for each Cartesian DOF. A perfect $1:1$ slope implies perfect tracking between reference and measured signals. These results demonstrate that multi-axial RTHS execution is both stable and



has good tracking. The hysteretic (force-deformation) plots for each DOF are shown in Fig. 14, indicating that the physical pier is tested into the nonlinear range.

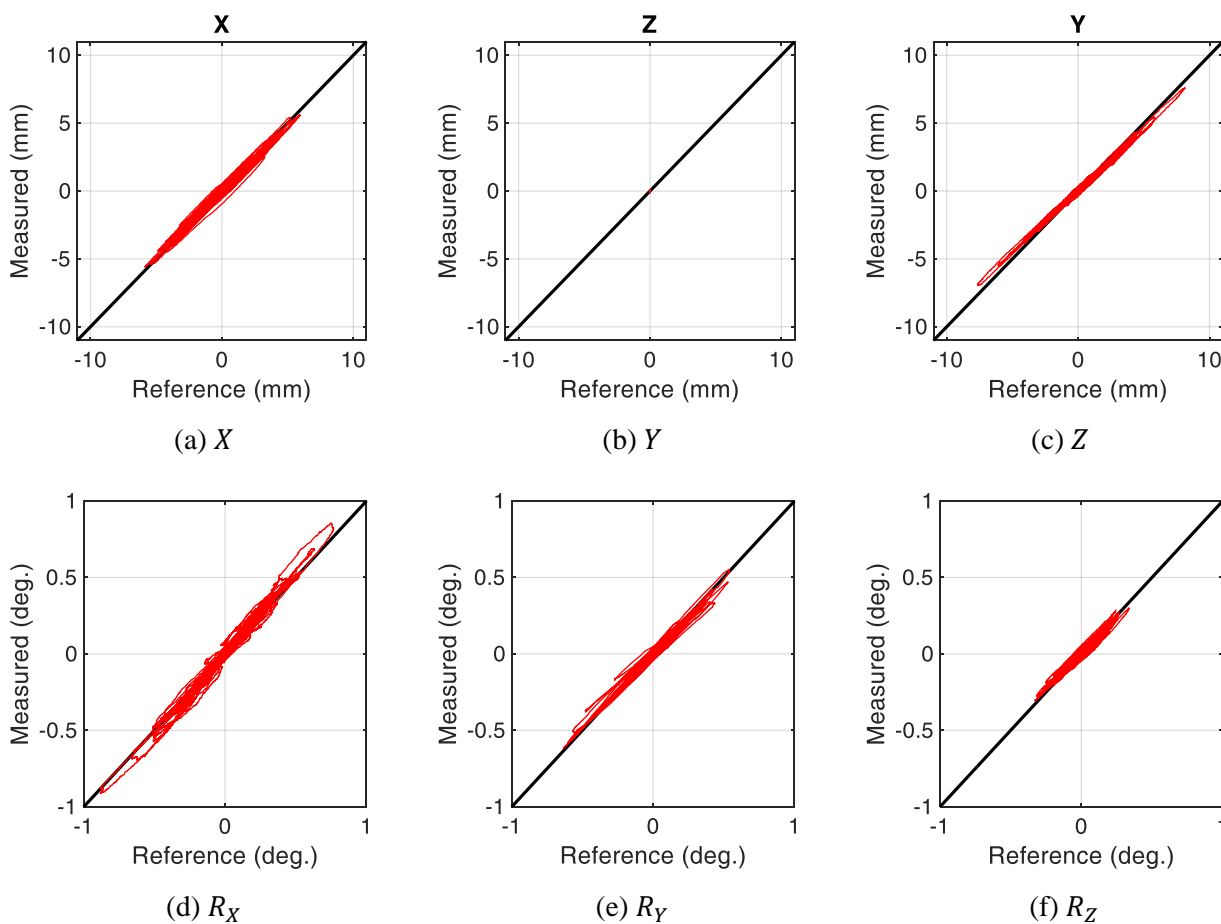
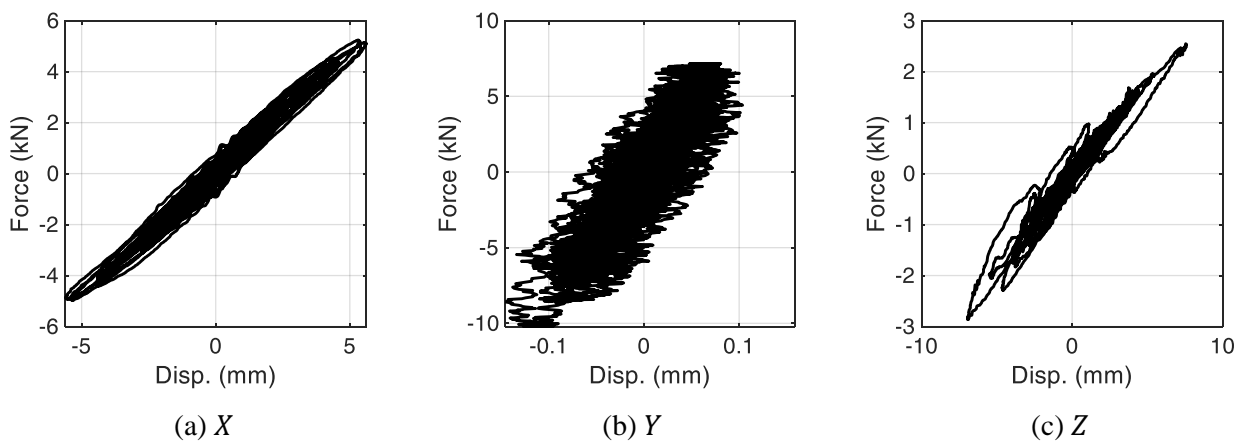


Fig. 13 Synchronization plots for the six Cartesian DOFs



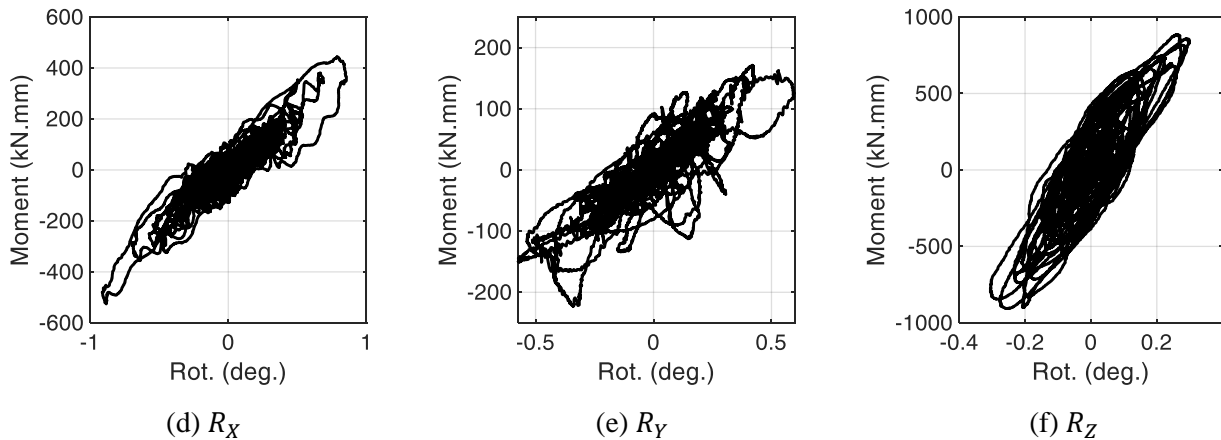


Fig. 14 Hysteretic behavior for the six DOFs

5. Conclusion

A framework for real-time hybrid simulation (RTHS) testing with multi-axial boundary conditions is proposed in this paper, comprised of four steps: (i) numerical substructure, (ii) numerical-to-physical transformation, (iii) physical substructure, and (iv) physical-to-numerical transformation. A decoupled control algorithm is proposed in the numerical-to-physical transformation, which compensates for the dynamics of each actuator channel independently. A 1/5th-scale Load and Boundary Condition Box (LBCB) device at the University of Illinois are chosen as the multi-axial boundary condition for verification of the proposed framework. The verification study is comprised of a multi-span curved bridge with 3 piers. The structure is partitioned into numerical and physical substructures. The physical structure is comprised of a round steel pier, fixed at the base and connected to the LBCB at the top. Results demonstrate a successful and stable execution of the multi-axial RTHS experiment. The results also highlight the promising nature of the multi-axial RTHS framework, as an alternative to existing means of testing structures under earthquake loading, including shake table testing and pseudo-dynamic methods.

6. References

- [1] M. Hakuno, M. Shidawara, and T. Hara, "Dynamic destructive test of a cantilever beam, controlled by an analog-computer," *Trans. Japan Soc. Civ. Eng.*, vol. 171, pp. 1–9, 1969.
- [2] K. Takanashi, K. Udagawa, M. Seki, T. Okada, and T. Tanaka, "Non-linear earthquake response analysis of structures by a computer-actuator on-line system (details of the system)," *Archit. Inst. Japan Trans.*, vol. 229, pp. 77–83, 1975.
- [3] M. Nakashima, H. Kato, and E. Takaoka, "Development of real-time pseudo dynamic testing," *Earthq. Eng. Struct. Dyn.*, vol. 21, no. August 1991, pp. 79–92, 1992.
- [4] T. Horiuchi, M. Nakagawa, M. Sugano, and T. Konno, "Development of a Real-time Hybrid Experimental System with Actuator Delay Compensation," *Proc. of 11th World Conf. Earthquake Engineering*. 1996.
- [5] J. E. Carrion, B. F. Spencer Jr., and B. M. Phillips, "Real-time hybrid simulation for structural control performance assessment," *Earthq. Eng. Eng. Vib.*, vol. 8, no. 4, pp. 481–492, 2009.
- [6] A. P. Darby, M. S. Williams, and A. Blakeborough, "Stability and delay compensation for real-time substructure testing," *J. Eng. Mech.*, vol. 128, no. 12, pp. 1276–1284, 2002.
- [7] B. M. Phillips and B. F. Spencer, "Model-Based Multiactuator Control for Real-Time Hybrid



Simulation,” vol. 139, no. February, pp. 219–228, 2013.

- [8] G. A. Fernandois and B. F. Spencer, “Model-based framework for multi-axial real-time hybrid simulation testing,” *Earthq. Eng. Eng. Vib.*, vol. 16, no. 4, pp. 671–691, 2017.
- [9] T. Horiuchi, M. Inoue, and T. Konno, “Development of a real-time hybrid experimental system using a shaking table,” *12th World Conf. Earthq. Eng.*, pp. 1–8, 2000.
- [10] A. Najafi and B. F. Spencer, “Modified model-based control of shake tables for online acceleration tracking,” *Unpubl. Manuscr.*, 2019.
- [11] A. Najafi, G. A. Fernandois, and B. F. Spencer, Jr., “Model-based real-time hybrid simulation with multi-axial load and boundary condition boxes,” *Under Rev.*, 2020.
- [12] T. Frankie *et al.*, “Hybrid simulation of curved four-span bridge,” in *Structures Congress*, 2013, pp. 721–732.